JOURNAL OF SOLID STATE CHEMISTRY 92, 213–218 (1991)

BRIEF COMMUNICATIONS

$Ba_2Fe_{10}Sn_2CoO_{22}$: Growth, Crystal Structure (120 K), and Magnetic Properties

F. SANDIUMENGE,* S. GALÍ,† R. RODRÍGUEZ-CLEMENTE, X. BATLLE,‡ AND X. OBRADORS

ICMAB, (CSIC), Martí i Franquès s/n, 08028 Barcelona, Spain; †Departament de Cristal.lografia i Mineralogia, U. B., Martí i Franquès s/n, 08028 Barcelona, Spain; and ‡Departament de Física Fonamental, U. B., Diagonal 647, 08028 Barcelona, Spain

Received July 31, 1990; in revised form December 3, 1990

We have grown single crystals of $Ba_2Fe_{10}Sn_2CoO_{22}$ in B_2O_3 flux. This phase is an isomorph of the novel K-type hexagonal ferrite. Using the starting composition we report here, a high yield of single crystals of the title compound is obtained as a unique phase over a wide cooling range. At 120 K the crystal structure has lattice parameters $a = 5.9316(7)$ and $c = 14.3128(32)$ Å, $Z = 1$, and space group $P\bar{3}$, although it has a strong $P\bar{3}m1$ pseudosymmetry. The Sn location in the crystal structure is discussed in terms of apparent valences calculated from bond strengths. In addition, the apparent valence provides insight into the Co^{2+} location. Our results are compared with those previously obtained by other authors using powdered samples of the same and structurally related compounds. A preliminary magnetic study points to behaviour consistent with that reported previously for polycrystalline samples.

After the work carried out by M. C. Cadée and D. J. W. Ijdo (*1*) the family of hexagonal ferrites was enlarged, introducing a new structural type. The crystal structure of the new group of compounds could not be represented by the previously known structural units (*2*) and a new building unit, the so-called Q-block, was described. The crystal structure is then described by the regular stacking of the Q and the spinel-like unit, the S-block. In this communication, we report the growth of single crystals of the title compound, and a structural and magnetic study, which is compared with the work carried out by Cadée *et al.* (*3*) using a polycrystalline sample and neutron diffraction.

Single crystals of the title compound were grown in the system BaO–CoO–B_2O_3–Fe_2O_3–SnO_2, 42.50, 6.53, 29.37, 15.07, 6.53 mol% by slow cooling (*4*). Starting materials were barium carbonate, cobalt acetate tetrahydrate, boron oxide, iron oxide, and tin oxide (Merck, pro analysis). The mixture was soaked at 1290°C and slowly cooled from 1260°C to 1000°C at -3°C h^{-1} in a platinum crucible. After cooling to room temperature, the crystals were separated from the solidified melt by dissolution in hot nitric acid. Crystals with mor-

* To whom correspondence should be addressed.

0022-4596/91 $3.00

TABLE I

FRACTIONAL COORDINATES ($\times 10^5$, M[a], Sn AND $\times 10^4$, O), POPULATION FACTORS, EQUIVALENT ISOTROPIC TEMPERATURE FACTORS[b] (Å^2), AND ANISOTROPIC TEMPERATURE COEFFICIENTS[c] ($\times 10^4$ Å^2) FOR $Ba_2M_{10.89(3)}Sn_{2.00(3)}O_{22}$ AT 120 K

Atom	Site	x/a	y/b	z/c	P_i	B_{eq}	U_{11}	U_{22}	U_{33}	U_{23}	U_{13}	U_{12}
Ba	2*d*	$\frac{1}{3}$	$\frac{2}{3}$	42,546(4)		0.67(3)	78(3)	78	100(4)	0	0	39
O(1)	2*c*	0	0	2,411(5)		—	59(13)					
O(2)	2*d*	$\frac{1}{3}$	$\frac{2}{3}$	903(5)		0.77(16)	84(20)	84	125(20)	0	0	42
O(3)	6*g*	1,556(7)	3,070(7)	9,153(3)		0.77(12)	138(15)	53(14)	103(16)	−8(12)	−8(13)	47(12)
O(4)	6*g*	4,952(8)	9,904(8)	2,451(3)		0.80(12)	142(15)	101(15)	86(16)	13(13)	0(13)	80(12)
O(5)	6*g*	1,738(7)	3,478(8)	5,909(3)		0.65(9)	100(5)	88(15)	77(14)	3(12)	−18(12)	59(12)
M(1)	2*d*	$\frac{1}{3}$	$\frac{2}{3}$	95,477(12)	0.977(2)	0.49(4)	59(5)	59	66(7)	0	0	30
M(2)	2*c*	0	0	37,557(11)	0.974(2)	0.49(4)	58(3)	58	69(8)	0	0	29
Sn(3)	2*d*	$\frac{1}{3}$	$\frac{2}{3}$	67,849(5)	0.946(2)	0.49(3)	57(3)	57	72(4)	0	0	28
M(3)					0.052(2)							
Sn(4)	1*a*	0	0	0	0.017(2)	0.55(6)	68(6)	68	71(10)	0	0	34
M(4)					0.981(2)							
Sn(5)	6*g*	16,987(15)	34,013(15)	17,273(7)	0.016(2)	0.62(4)	85(5)	61(4)	88(5)	1(3)	−2(3)	35(4)
M(5)					0.984(2)							

[a] M = Fe + Co.
[b] $B_{eq} = (\frac{8}{3})\pi^2\Sigma_i\Sigma_j U_{ij}a_i^*a_j^*a_i \cdot a_j$.
[c] Based on the exponential expression $-2\pi^2(h^2a^{*2}U_{11} + k^2b^{*2}U_{22} + l^2c^{*2}U_{33} + 2hka^*b^*U_{12} + 2hla^*c^*U_{13} + 2klb^*c^*U_{23})$.

phology consisting of a combination of hexagonal prism, rombohedron (prominent faces), and pinacoid were obtained. The chemical composition deduced from energy dispersive X-ray (EDX) analyses and corrected for Z.A.F. (ZAF-4/FLS, Link Systems Ltd.) is 47.7 ± 0.6 Fe_2O_3, 10.0 ± 0.8 CoO, 22.0 ± 0.5 SnO_2, and 20.3 ± 0.4 BaO mol%. Metallic Fe, Co, and Sn, and $BaSO_4$ were used as standards (C. M. Taylor Corp.). Some analyses performed on a polished plane perpendicular to the basal face of a single crystal indicated homogeneity in composition within experimental accuracy.

Data collection was performed on an Enraf–Nonius CAD-4 diffractometer using a single crystal sphere of radius 0.15 mm, with the Mo$K\alpha$ graphite monochromated radiation. In order to achieve better accuracy, the spectrum was recorded at 120 K, by immersion of the sample in blowing nitrogen gas. The lattice constants obtained at the above temperature from 25 reflections with $13.8° \leq \Theta \leq 32.7°$ are a = 5.9316(7) and c = 14.3128(32) Å. A total of 1582 reflections were measured within $-7 \leq h, k \leq 7$ and $0 \leq l \leq 17$, $1 \leq \Theta \leq 25$, by a $\omega - 2\Theta$ scan mode. Spherical absorption (μR = 2.34) was corrected numerically according to the $A^*(\Theta)$ values available in Ref. (*5*). After a Patterson synthesis the location of Ba and (M + Sn)(3) cations (Table I) was deduced. Almost all the remaining sites were generated with DIRDIF (*6*). First attempts of refining with the space group $P\bar{3}m1$ (No. 164) resulted systematically in negative O(1) isotropic thermal parameters and an erratic progression of the R factors. Finally, the spectrum was reduced in the $\bar{3}$ Laue class and the space group $P\bar{3}$ (No. 147), Z = 1, was adopted. The crystal structure was refined with 403 unique reflections with $I > 5\sigma(I)$, using the SHELX 76 program (*7*). The refinement converged to R = 0.0325 and R_w = 0.0367. The final difference electron density distribution has a minimum and a maximum at −1.6 and 1.23 eÅ^{-3}. In Table I the refined fractional atomic coordinates, M = Fe + Co and Sn population factors, P_i, and anisotropic temperature coefficients are given. It is seen that deviations from the special position x,

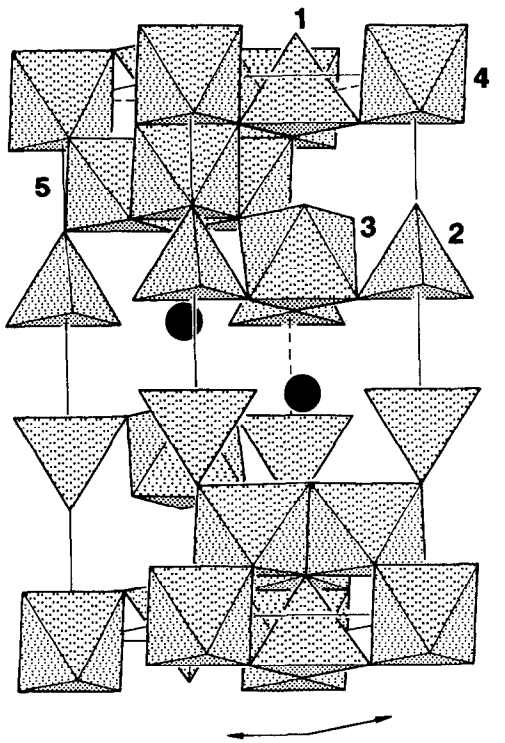

FIG. 1. Perspective view of the content of a unit cell observed approximately normal to the *ac* plane, with the *c* axis vertical. The numbers from 1 to 5 refer to the designation used in the text for each cation in a particular crystallographic site. Black circles represent Ba atoms.

$2x$, z are only significance for O(3), $y - 2x = -0.0042(7)$, amounting to only twice the standard deviation for (M + Sn)(5). This indicates that a strong $P\bar{3}m1$ pseudosymmetry holds. The refined chemical formula is $Ba_2M_{10.89(3)}Sn_{2.00(3)}O_{22}$, M = Fe + Co, in good agreement with the expected nominal composition. However, the refined occupation of tetrahedral sites deviates by 2.4(2)% from full occupation.

Figure 1 shows a perspective view of the structure. The main feature is the existence of a double BaO_3 layer in the Q-block. At the level of the double BaO_3 layer no interstices are occupied. In consequence, the density of polyhedral packing is highly reduced at this level, as compared for instance with the R-block (*8*). Figure 2 shows the coordination polyhedra of the different cations, and in Table II interatomic distances within each coordination polyhedra are given.

With regard to the site preference of the Sn, a high degree of Sn ordering in the 2*d* octahedra (*atom(3)*), adjacent to the double BaO_3 (Q-block), is observed: 94.6(2) at%

TABLE II

CATION–OXYGEN DISTANCES (Å) FOR THE COORDINATION POLYHEDRA

Ba cuboctahedron (Q block)	
O(4)–Ba:	3.068(4) ×3
O(5)–Ba:	2.876(5) ×3
O(5)–Ba:	2.971(5) ×6
⟨O–Ba⟩:	2.971(5)
***M*(1) tetrahedron (S block)**	
O(2)–*M*(1):	1.939(8) ×1
O(3)–*M*(1):	1.928(4) ×3
⟨O–*M*(1)⟩:	1.931(5)
***M*(2) tetrahedron (Q block)**	
O(1)–*M*(2):	1.924(7) ×1
O(5)–*M*(2):	1.847(6) ×3
⟨O–*M*(2)⟩:	1.866(6)
(*M* + Sn)(3) octahedron (Q block)	
O(5)–(*M* + Sn)(3):	2.060(4) ×3
O(4)–(*M* + Sn)(3):	2.070(5) ×3
⟨O–(*M* + Sn)(3)⟩:	2.065(5)
(*M* + Sn)(4) octahedron (S block)	
O(3)–(*M* + Sn)(4):	1.987(4) ×6
(*M* + Sn)(5) octahedron (Q–S interphase)	
O(1)–(*M* + Sn)(5):	2.000(3) ×1
O(2)–(*M* + Sn)(5):	2.048(5) ×1
O(3)–(*M* + Sn)(5):	2.079(4) ×1
O(3)–(*M* + Sn)(5):	2.098(5) ×1
O(4)–(*M* + Sn)(5):	1.964(5) ×2
⟨O–(*M* + Sn)(5)⟩:	2.025(5)

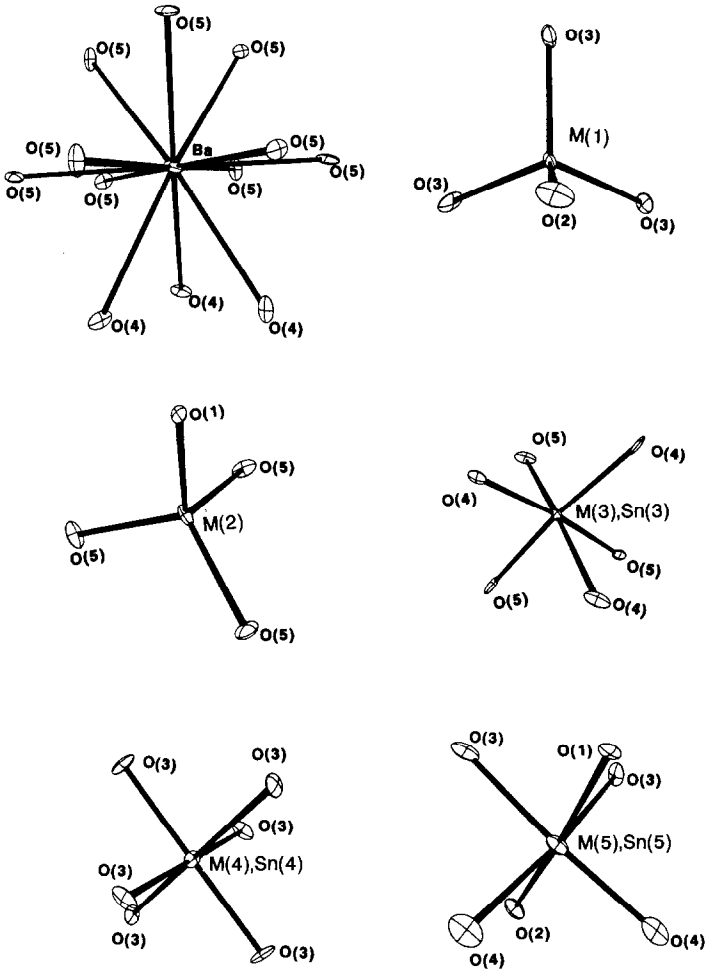

FIG. 2. Coordination polyhedra for each cation in the refined $Ba_2M_{10.89(3)}Sn_{2.00(3)}O_{22}$, M = Fe + Co, crystal structure. Ba: cuboctahedron bounded by three O(4) atoms and nine O(5) atoms. The Ba position is slightly deviated from the plane of O(5) atoms by 0.01636(17)c Å. M(1): tetrahedron shown approximately normal to the ab plane, the three basal O(3) atoms are shared with 1a and 6g octahedra, and O(2) with 6g octahedron. M(2): tetrahedron bounded by three O(5) atoms lying on a plane parallel to ab, shared with 2d octahedra, and an O(1) atom shared with a 6g octahedron. Cation(3): octahedral coordination as observed normal to the ab plane. Cation (4): octahedral coordination with all cation–O(3) distances equivalent. Cation(5): octahedral coordination. The two cation–O(3) distances are different. This site is located at the Q–S interphase.

Sn. Cadée *et al.* (*3*) reported (85.3(21) at% Sn. Our results indicate that the excess of Sn is distributed almost equally among the remaining octahedral sites (Table I). Confirmation of this observation was reinforced by the calculation of apparent valences. The apparent valences, calculated from bond strengths Σ_{calc}, are summarized in Table III. The Σ_{calc} for (M + Sn)(4) and (M + Sn)(5) atoms, calculated on the basis of 100 at% Fe at both sites, are consistent with some degree of Sn location at the 1a octa-

TABLE III

BOND VALENCE SUMMATIONS FOR CATIONS IN $Ba_2M_{10.89(3)}Sn_{2.00(3)}O_{22}$[a]

	O(1)	O(2)	O(3)	O(3)	O(4)	O(5)	O(5)	Σ_{calc}[b]
Ba					0.120 ×3	0.202 ×3	0.156 ×6	1.91
M(1)		0.615 ×1	0.633 ×3					2.51
M(2)	0.640 ×1					0.788 ×3		3.00
(*M* + Sn)(3)					0.640 ×3	0.658 ×3		3.89
(*M* + Sn)(4)			0.540 ×6					3.24
(*M* + Sn)(5)	0.520 ×1	0.458 ×1	0.421 ×1	0.400 ×1	0.575 ×2			2.95

[a] Based on the assumption of 100% Sn at (*M* + Sn)(3) and 100% Fe at the remaining sites.
[b] $\Sigma_{calc} = \Sigma_j \exp[(r_0 - r_{ij})/b]$, data from Ref. (*10*); r_{ij} values are listed in Table II.

hedra (*atom(4)*), in contrast with the results of Cadée *et al.* (*3*), who stated that no Sn is located at these sites. On the other hand, these values are indicative of some Co^{2+} location at the edge-sharing 6*g* octahedra (*atom(5)*). According to recent results of Co and Sn distribution in barium ferrites with the magnetoplumbite structure (*9*), in the octahedral sites, Co^{2+} is located in the face sharing $4f_{vi}$ and edge sharing 12*k* (equivalent to 6*g*) and does not enter the 2*a* octahedra (equivalent to 1*a*) at all.

In tetrahedral sites, the situation becomes easier since no Sn is present. Our low Σ_{calc} values for *M*(1) cations (2*d* tetrahedra) prove that this site is occupied by Co^{2+} to a large extent, as stressed by Cadée *et al.* (*3*) for this phase and other authors for other Co^{2+} containing hexagonal ferrites (*11*). On the contrary, the *M*(2) cation may be regarded as 100 at% Fe, also in good agreement with those authors.

To characterize this crystal further, isothermal magnetization measurements were performed with a SQUID magnetometer (Quantum Design) in fields up to 5 T. The external field was oriented perpendicular to the *c* axis and the curves were recorded in a decreasing magnetic field. A typical experimental curve and a representation of the calculated derivative *dM/dH* are shown in Figs. 3 and 4. As it is clear from these curves a prominent anomaly is observed at about 12.5 kOe and a tendency to saturation is evidenced at high fields but definitely no block–metamagnetic transition is observed below 5 T, as reported by Cadée *et al.* (*3*) in polycrystalline samples.

Our preliminary magnetic investigation of the present $Ba_2Fe_{10}Sn_2CoO_{22}$ single crystals points to a behavior consistent with that reported previously for polycrystalline samples (*3*). These authors reported a block–metamagnetic transition at high magnetic fields which they associated to a weakening of the antiferromagnetic superexchange interactions along the *c* axis at

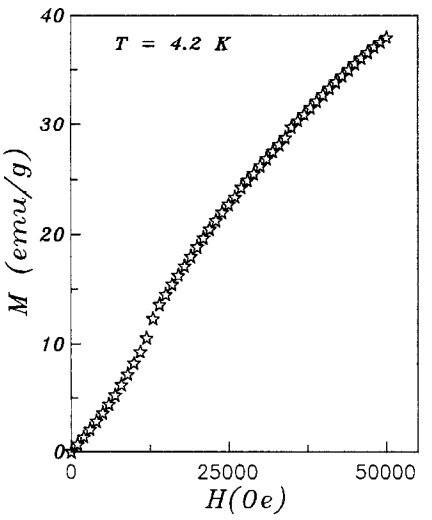

FIG. 3. *M*(*H*) curves recorded at 4.2 K with $H \| ab$.

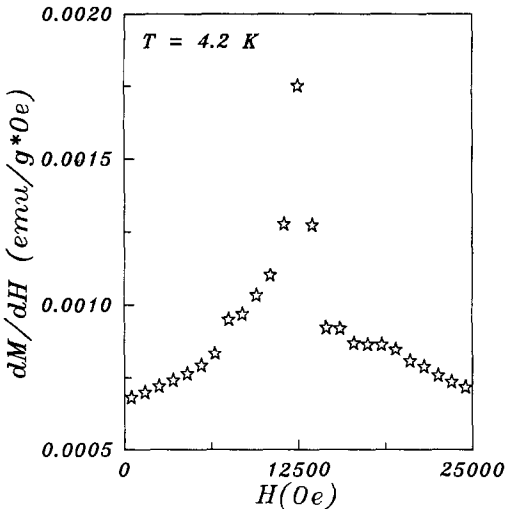

FIG. 4. Calculated dM/dH derivative versus H.

the level of the double BaO_3 layer. This magnetic interaction is indeed of super–superexchange character and thus this weakening should be expected. It should be mentioned as well that the situation becomes even worse when we consider that the (M + Sn)(3) octahedra have an important concentration of nonmagnetic Sn ions and thus the responsibility of the interblock magnetic coupling is only associated with the magnetic ions located in the $M(2)$ tetrahedra.

The magnetization measured on our single crystal is slightly lower than that reported in polycrystalline samples (*3*) and this is indeed consistent with the expected antiferromagnetic susceptibility anisotropy. On applying $\mathbf{H} \perp c$, and staying below the metamagnetic-like transition, the magnetic field remains parallel to the magnetic moments and thus the low temperature susceptibility is small.

Now the observed anomaly in dM/dH at about 12.5 KOe (Fig. 4) should be understood in terms of the displacement of antiferromagnetic domains. Actually, because of the mixed distribution of magnetic and nonmagnetic cations within the structure, small noncompensated magnetic moments will exist in each antiferromagnetic domain. When a magnetic field is applied within the a–b plane the small planar anisotropy is overcome and thus the domains suffer a reorientation.

A full study of the anticipated complex magnetic behavior of this system is now underway on higher magnetic fields in order to study the metamagnetic-like transition.

Acknowledgment

This work was supported by the CICYT, Project MAT88-0259.

References

1. M. C. CADÉE AND D. J. W. IJDO, *J. Solid State Chem.* **40,** 290 (1981).
2. J. A. KOHN, D. W. ECKART, AND C. F. COOK, JR., *Science* **172,** 519 (1971).
3. M. C. CADÉE, H. J. M. DE GROOT, L. J. DE JONGH, AND D. J. W. IJDO, *J. Magn. Magn. Mater.* **62,** 367 (1986).
4. F. SANDIUMENGE, S. GALÍ, AND R. RODRÍGUEZ-CLEMENTE, *J. Crystal Growth,* in press.
5. International Tables for X-Ray Crystallography, Kynoch Press, Birmingham, Vol. II, 302 (1974).
6. P. T. BEURSKEN *et al.*, DIRDIF Tech. Rep. 1984/1 Crystallography Laboratory, Univ. of Nijmegen 1984.
7. G. M. SCHELDRICK, "SHELX76 Program for Crystal Structure Determination," Univ. of Cambridge, England (1976).
8. F. VON HABEREY AND M. VELICESCU, *Acta Crystallogr. Sect. B* **30,** 1507 (1974).
9. X. BATLLE, Tesis Doctoral. Universitat de Barcelona (1990).
10. I. D. BROWN AND D. ALTERMATT, *Acta Crystallogr. Sect. B* **41,** 244 (1985).
11. A. COLLOMB, B. LAMBERT-ANDRON, J. X. BOUCHERLE, AND D. SAMARAS, *Phys. Status Solidi A* **96,** 385 (1986). A Collomb, M. A. Hadj, and J. C. Joubert, *Mater. Res. Bull.* **24,** 453 (1989).